Heliyon 8 (2022) e09472

Contents lists available at ScienceDirect

Heliyon

journal homepage: www.cell.com/heliyon

Research article

Silver nanoparticles synthesized by the heavy metal resistant strain *Amycolatopsis tucumanensis* and its application in controlling red strip disease in sugarcane

Daiana S. Guerrero [a,1], Romina P. Bertani [b,1], Ana Ledesma [c,d], M. de los Angeles Frías [c], Cintia M. Romero [a,e], José S. Dávila Costa [a,*]

[a] *Planta Piloto de Procesos Industriales Microbiológicos- (PROIMI-CONICET), Av. Belgrano y Pasaje Caseros, T4001 MVB, Tucumán, Argentina*
[b] *Estación Experimental Agroindustrial Obispo Colombres – Sección Fitopatología, Av. William Cross 3150, T4101 XAC, Tucumán, Argentina*
[c] *Centro de Investigación en Biofísica Aplicada y Alimentos (CIBAAL-UNSE-CONICET), Universidad Nacional de Santiago del Estero, R N N° 9, Km 1125, El Zanjon, 4206, Santiago del Estero, Argentina*
[d] *Departamento Académico de Química, Facultad de Ciencias Exactas y Tecnologías, Universidad Nacional de Santiago del Estero (UNSE), Av. Belgrano Sur 1912, 4200, Santiago del Estero, Argentina*
[e] *Facultad de Bioquímica, Química y Farmacia, Universidad Nacional de Tucumán (UNT), Ayacucho 471, T4001 MVB, Tucumán, Argentina*

ARTICLE INFO

Keywords:
Silver nanoparticles
Antibacterial effect
Acidovorax avenae subsp. *avenae*
Red stripe disease
Sugarcane

ABSTRACT

The production of bioethanol and sugar from sugarcane is an important economic activity in several countries. Sugarcane is susceptible to different phytopathogens. Over the last years, the red stripe disease caused by the bacterium *Acidovorax avenae* subsp. *avenae* produced significant losses in sugarcane crops. Bio-nanotechnology emerged as an eco-friendly alternative to the biosynthesis of antimicrobial molecules. The aims of this study were to (a) produce extracellular silver nanoparticles using the heavy metal resistant strain *Amycolatopsis tucumanensis*, (b) evaluate their antibacterial *in vitro* effect and (c) determine the potential of silver nanoparticles to protect sugarcane against red stripe disease.

Amycolatopsis tucumanensis synthesized spherical silver nanoparticles with an average size of 35 nm. Nanoparticles were able to control the growth of *A. avenae* subsp. *avenae* in *in vitro* assays. In addition, *in vivo* assays in sugarcane showed a control upon the red stripe disease when silver nanoparticles were applied as preventive treatment. The Disease Severity Index was 28.94% when silver nanoparticles were applied 3 days before inoculation with *A. avenae* subsp. *avenae*. To our knowledge, this is the first report of silver nanoparticles extracellularly synthesized by an *Amycolatopsis* strain that were able to inhibited the growth of *A. avenae* subsp. *avenae* and control the red stripe disease in sugarcane.

1. Introduction

Green biotechnology encompasses the use of technologies to produce more productive crops and ensures the application of environmentally friendly fertilizers and biopesticides (Kafarski, 2012). Sugarcane industry was traditionally focused in the production of sugar. Since the incorporation of the concept of biorefinery into the industry, sugar mills started to produce bioethanol. For instance, the production of bioethanol from sugarcane in Argentina was at 980 million liters in 2021 ("Argentina: Biofuels Annual | USDA Foreign Agricultural Service," n.d.). Sugarcane is susceptible to several bacterial diseases such as the red stripe caused by the bacterium *Acidovorax avenae* subsp. *avenae* (Rott and Davis, 2000). In the last decade, a significant increase in the prevalence and incidence of red stripe disease was observed, especially in the North of Argentina (Bertani et al., 2021; Fontana et al., 2013). Actually, several sugarcane producing regions worldwide were affected by this disease (Brigida et al., 2016; Yonzone and Soniya Devi, 2018; Zhou et al., 2021).

The increasing use of pesticides promoted the occurrence of highly resistant phytopathogens (Ramakrishnan et al., 2019). In 2019, approximately 3.5 million tons of pesticide were used worldwide causing a negative impact in the environment and human health (Sharma et al.,

* Corresponding author.
E-mail address: jsdavilacosta@gmail.com (J.S. Dávila Costa).
[1] Equal contribution.

https://doi.org/10.1016/j.heliyon.2022.e09472
Received 21 January 2022; Received in revised form 13 April 2022; Accepted 13 May 2022

2019). Undoubtedly, eco-friendly molecules are needed to the control of the phytopathogens.

Nanobiotechnology is a field that introduces special biological properties of nanostructures and their application in areas such as medicine and agriculture (Asghari et al., 2016; Kumar et al., 2021). Particularly, the antimicrobial activity of silver nanoparticles has been evaluated in the last years.

Among the synthesis techniques used, the biological synthesis of silver nanoparticles emerged as an interesting environmental-friendly alternative (Bansal et al., 2017a, 2017b; Eid et al., 2020; Paterlini et al., 2021).

The biogenic synthesis of nanoparticles depends on the activity of reductase enzymes (Rai et al., 2011; Sindhu et al., 2015). In this process, a heavy metal ion such as Ag^{+} is reduced to the metallic form Ag^{0} and it is stabilized by organic molecules produced by the microorganism. Several mechanisms involved in the biosynthesis of nanoparticles were proposed (Saravanan et al., 2021; Wanarska and Maliszewska, 2019). The phylum *Actinobacteria* is recognized for encompassing biotechnologically important genera such as *Amycolatopsis* (Dávila Costa and Amoroso, 2014). Some strains are known to produce important antibiotics such as rifamycin and vancomycin among others (Jeong et al., 2013; Verma et al., 2011; Xu et al., 2018). The strain *Amycolatopsis tucumanensis,* that belongs to the family *Pseudonocardiaceae* (Goodfellow, 2012), was mainly reported for its ability to reduce copper and bioremediate polluted soils (Albarracín et al., 2010; Dávila Costa et al., 2011). Moreover, several studies support the hypothesis that *A. tucumanensis* is an environmental strain that may be used for the green synthesis of silver nanoparticles (Albarracín et al., 2010; Bourguignon et al., 2016, 2019; Dávila Costa et al., 2012, 2011). So far, the biogenic synthesis of nanoparticles was not reported in this genus.

The aims of this study were to (a) produce extracellular silver nanoparticles using the heavy metal resistant strain *A. tucumanensis*, (b) evaluate their antibacterial *in vitro* effect and (c) determine the potential of silver nanoparticles to protect sugarcane against red stripe disease.

2. Materials and methods

2.1. Microorganism, culture media

Amycolatopsis tucumanensis AB0 DSM 45259 isolated from copper-polluted sediments was used in this work (Albarracín et al., 2005). *A. tucumanensis* was grown in ISP-2 culture medium (International *Streptomyces* Production-2), g/L: Peptone, 5; Yeast extract, 3; Malt extract, 3; Dextrose, 10, pH 7; or Minimal Medium (MM), g/L: NH_4SO_4, 4; K_2HPO_4, 0.5; $MgSO_4$ $7H_2O$, 0.2; $FeSO_4$ $7H_2O$, 0.01; pH 7.

2.2. Biosynthesis of silver nanoparticles

One hundred mL of ISP-2 medium were inoculated with a single colony of *A. tucumanensis* and incubated at 30 °C, 150 rpm for 72 h. Afterward, cells were harvested by centrifugation (10,000 x *g*, 15 min) and the purified cell-free supernatant was used for the biosynthesis. Nitrate reductase activity of the cell-free supernatant was determined according to the protocol described by Vaidyanathan et al. (2010). $AgNO_3$ was added to the cell-free supernatant to a final concentration of 0.5, 1, 2 and 3 mM and incubated in the dark at 30 °C and 150 rpm for 24, 48 and 72 h. The success of the biosynthesis was assessed by scanning the absorbance (300–750 nm) in a UV–visible spectrophotometer (Thermo Scientific Multiskan SkyHigh). In addition, the change of color into yellowish-brown that indicates the formation of silver nanoparticles (AgNPs) was monitored. The synthesized AgNPs were harvested by centrifugation (10,000 x *g*, 10 min), washed, resuspended in distilled water and stored at 8 °C. The concentration of AgNPs was determined by Inductively Coupled Plasma Optical Emission Spectroscopy (ICP-OES) (Shimadzu). ISP-2 medium amended with $AgNO_3$ was used as abiotic control. The same protocol was used for the synthesis of nanoparticles in Minimal Medium.

2.3. Characterization of silver nanoparticles

Scanning Electron Microscopy (SEM) (JEOL JSM-35 CF) was used to assess the shape and size of the AgNPs. Additionally, the elemental composition was analyzed by Energy-Dispersive Spectroscopy (EDS) (Inca Penta FET X3, Oxford instrument). Molecular structure and chemical bonds of AgNPs were detected by Raman Spectroscopy (LabRAM HR Evolution Raman microscope) and Fourier Transform Infrared (FTIR) (Thermo Scientific 6700 spectrometer assembled with an ATR accessory with temperature chamber control, and deuterated triglycine sulfate (DTGS) KBr detector, connected to a system of circulation of dry air to avoid the interference of water vapor and carbon dioxide). Potential zeta was measured in order to determine the stability of the AgNPs after one month of storage in distilled water. The hydrodynamic diameter of AgNPs was measured in a dynamic light scattering (DLS) SZ-100 Horiba. The detection angle was 173° and DLS measurements were conducted with a fixed 100 runs andeach run lasts 30 s. X-ray diffraction (XRD) pattern of dry AgNPs powder was obtained using a Rigaku Miniflex 300 X-ray diffractometer with $\lambda_{Cu} = 1{,}5418$ nm.

2.4. In vitro antimicrobial activity of AgNPs against phytopathogens

Antimicrobial activity of AgNPs was tested against the bacterial sugarcane phytopathogen *Acidovorax avenae* subsp. *avenae*. The strain was provided by the Estación Experimental Agroindustrial Obispo Colombres (EEAOC), Tucumán-Argentina.

The effect of AgNPs against *A. avenae* subsp. *avenae* was evaluated by the well-diffusion method and subsequently the minimal inhibitory concentration (MIC) was determined (Wiegand et al., 2008). For the well-diffusion method, *A. avenae* subsp. *avenae* was grown in Mueller Hinton (MH) broth up to OD_{600} of 0.1 (10^8 CFU/mL) and 100 μl of the bacterial suspension were plated onto MH-agar. Then, 9 mm diameter wells were made and filled with 100 μl of AgNPs. Plates were incubated at 37 °C for 24 h. Inhibition halos (mm) were measured using a millimeter scale and the mean value was recorded. Results are presented as the mean of three biological independent replicates. The MIC for *A. avenae* subsp. *avenae* was determined according to the Broth Dilution Method described by Wiegand et al. (2008) (see Supplementary materials). ISP-2 medium and the cell-free supernatant with secondary metabolites produced by *A. tucumanensis* were used as control for antimicrobial activity. Results are presented as the mean of three biological independent replicates. Statistical analyses were performed with the software Microcal Origin 6.0.

2.5. In vivo control evaluation of AgNPs against Acidovorax avenae subsp. avenae

2.5.1. Plant material and growing conditions

The plants of red stripe susceptible cultivar TUC 00–19 (Cuenya et al., 2013) produced from healthy single-bud sets of sugarcane in the greenhouse were planted in 1L pots containing a commercial substrate (Grow mix Multipro). Sugarcane plants were grown under greenhouse conditions until use. The plants were 60–70 days old with about four leaves completely lifted at the time of the experiment and were fertilized with 120 kg/ha of Nitrodoble according to Bertani et al. (2020), ten days prior to silver nanoparticles treatment.

2.5.2. Silver nanoparticles assay against sugarcane red stripe disease

Four treatments were evaluated in order to analyze the induced resistance (applications before pathogen inoculation) and/or the antibacterial effect (applications after pathogen inoculation) of AgNPs against *A. avenae* subsp. *avenae* (Table 1). The assays were performed according to the protocol described by Chalfoun et al. (2018). Mock,

Table 1. Red stripe disease severity index and area under disease progress curve values from sugarcane assay during three evaluation times.

Treatments	Application timing	Disease Severity Index (%)			AUDPC****
		5 dai	7 dai	9 dai	
T1-Mock	-	40.11b***	46.25ab	39.90a	272.79b
T2- AgNPs	3 dbi*	34.07b	41.00a	28.94b	230.29c
T3- AgNPs	2 dai**	40.70b	43.08a	38.24a	266.85bc
T4- AgNPs	5 dai	47.59a	50.49a	43.32a	310.87a
P =		0.0086	0.1177	0.0015	0.0091

Mock: positive infection control.
AgNPs: silver nanoparticles.
* days before inoculation.
** days after inoculation.
*** Means in each column followed by the same letter are not significantly different (LSD, $P = 0.05$).
**** Area under disease progress curve.

water-treated plants were used as positive infection control (T1). AgNPs were applied 3 days before pathogen inoculation (T2). In addition, AgNPs were applied 2 and 5 days after pathogen inoculation (T3 and T4, respectively). Not infected plants were used as negative control. Silver nanoparticles were applied by spraying plants to run-off. For pathogen infection, a virulent isolate of *A. avenae* subsp. *avenae* was grown on nutrient broth (NB) and a suspension containing 10^8 CFU/mL was prepared (Bertani et al., 2020). Afterwards, the inoculum was applied by spraying the adaxial and abaxial surfaces of sugarcane leaves until run-off with a manual atomizer. Infected plants were kept at 30 °C and 100% relative humidity (RH) (covered with a plastic bag) for the first 24 h. Then, a RH >80% was maintained until the end of the assay (Bertani et al., 2020).

2.5.3. Experimental design and red stripe assessment

Mock-treated plants (water) were used as positive disease control. Plants were arranged in a randomized complete block design and 20 sugarcane plants (biological replicates) were used for each treatment. Red stripe severity was evaluated on all leaves of each plant at 5, 7 and 9 days post inoculation (dpi) according to the International Society of Sugarcane Technologists scale ranging from 0 (no disease) to 9 (more than 50% of the foliar area affected by the disease) (Bertani et al., 2020). The leaf affected areas (%) were adjudicated to the following disease severity classes: 0 (0%), 1 (<0.5%), 2 (0.5%), 3 (1%), 4 (5%), 5 (10%), 6 (25%), 7 (35%), 8 (50%), or 9 (>50%).

Disease severity index of red stripe (DSI) was calculated from the scores of the leaves for each plant and treatment using the formula: $DSI = \sum(A \times 0 + B \times 1 + C \times 2 + D \times 3 + E \times 4 + F \times 5 + G \times 6 + H \times 7 + I \times 8 + J \times 9)/(T \times 9) \times 100$. A to J are the number of leaves corresponding to the numerical severity grade from 0 to 9, respectively, and T is the total number of leaves.

Data adjustment, variance analysis and means comparison for each treatment were performed by Infostat package version 2018 (Di Rienzo et al., 2018), using Lineal Mixed General Models. Area under the disease progress curve (AUDPC) was determined, using the DSI, following a trapezoidal integration model (Campbell, 1990). Means of DSI at each time and AUDPC were compared among treatments by LSD Fisher test at the 0.05 significance level and grouping was indicated with letters (Table 1).

3. Results and discussion

3.1. Synthesis of extracellular silver nanoparticles by A. tucumanensis

The synthesis of AgNPs was evaluated in ISP-2 and Minimal culture media. The synthesis of biological AgNPs was achieved after 72 h of incubation by activity of the metabolites released by *A. tucumanensis*. The change of color into yellowish-brown and the absorbance of the surface plasmon resonance located at 405 nm suggested the green synthesis of AgNPs (Figure 1 A, B and C) similar to the reported of another authors (Jalab et al., 2021; Rodríguez-Félix et al., 2021). In the abiotic control (ISP-2 + $AgNO_3$) neither change of color nor plasmon formation were observed. AgNPs were not synthesized in MM.

The extracellular synthesis of AgNPs in *A. tucumanensis* was carried out in the presence of 0.5 and 1 mM of $AgNO_3$ (Fig. 1B and C). The UV-VIS spectra showed defined peaks for the surface plasmon resonance of the AgNPs and the absorbance increased with the incubation time. In the presence of 2 and 3 mM of $AgNO_3$ the formation of the plasmon resonance was not observed. In contrast to *A. tucumanensis*, recent studies reported the extracellular synthesis of AgNPs by *Bacillus* strains using higher concentrations (between 3 and 5 mM) of $AgNO_3$. The absorption peaks for the surface plasmon resonance in these *Bacillus* strains were broad and less defined (Ahmed et al., 2020; Ibrahim et al., 2020). Numerous reports postulated that the wider the plasmon peak, the greater the dispersion of nanoparticles size (Golinska et al., 2017; Roy et al., 2019; Zhang et al., 2020).

Several mechanisms for the biosynthesis of nanoparticles were proposed (Jalab et al., 2021; Rodríguez-Félix et al., 2021; Saravanan et al., 2021). In the synthesis of AgNPs, the reduction of Ag^+ ions is attributed to the combined action of bio-molecules such as proteins, vitamins, lipids, etc, produced by the bacteria. The most accepted mechanism involves the enzyme nitrate reductase. This enzyme reduces the nitrate (NO_3^-) to nitrite (NO_2^-) and the resulting electron is transferred to the Ag^+ ion to form metallic silver (Ag^0) (Rai et al., 2011; Roy et al., 2019; Sindhu et al., 2015). The cell-free supernatant of *A. tucumanensis* showed a nitrate reductase activity of 291 U/mL.

Similar to other filamentous *Actinobacteria* such as *Streptomyces*, the biotechnological potential of the genus *Amycolatopsis* relies on the wealth of its secondary metabolites and the extracellular metabolism (Dávila Costa and Amoroso, 2014). *A. tucumanensis* was widely study for its ability to remove copper from soils. The resistance mechanisms of this strain include an efficient antioxidant system, metallothioneins that bind copper and the extracellular reduction of Cu^{2+} (Dávila Costa et al., 2011; Dávila Costa et al., 2012).

Often, bacterial reductase enzymes are not specific. In the present work, Ag^+ was extracellularly reduced as evidenced by the formation of nanoparticles in the cells-free supernatant. This result suggest that the extracellular enzymes of *A. tucumanensis* not only may reduce Cu^{2+} in bioremediation processes but also Ag^+ for the synthesis of bio-nanoparticles. The extracellular synthesis of bionanoparticles represents an advantage for further downstream processes. For instance, the extraction and purification of the AgNPs could be performed in few steps or not even needed.

3.2. Physicochemical properties of the silver nanoparticles produced by A. tucumanensis

The antimicrobial capacity of nanoparticles often depends on their size. In general, smaller the nanoparticle, higher antimicrobial activity was observed (Golinska et al., 2017). DLS and SEM studies showed that most of the AgNPs had a size of 35 nm and were mostly spherical (Figures 2A and 2B). EDS analysis showed 40.4% of silver in the nanoparticle composition. The optical absorption band observed for the plasmon resonance at about 405 nm (Figure 1B) and the signal for elemental silver (3–4 keV) in the EDS spectrum (Figure 2C) were consistent with the absorption of metallic silver nanocrystallites (El-Naggar et al., 2014; Magudapathy et al., 2001). The peaks for carbon (34.6%), oxygen (19.4%) and other minor elements in the EDS spectrum suggested the presence of organic molecules associated to the AgNPs.

The XRD pattern obtained for the AgNPs is shown in Figure 3. The Bragg reflection peaks representative of the face centered cubic (fcc) of silver nanocrystals were observed (111, 200, 220 and 311 facets) (Figure 3) (Philip 2009; Shankar et al., 2003; Singh et al., 2021). The

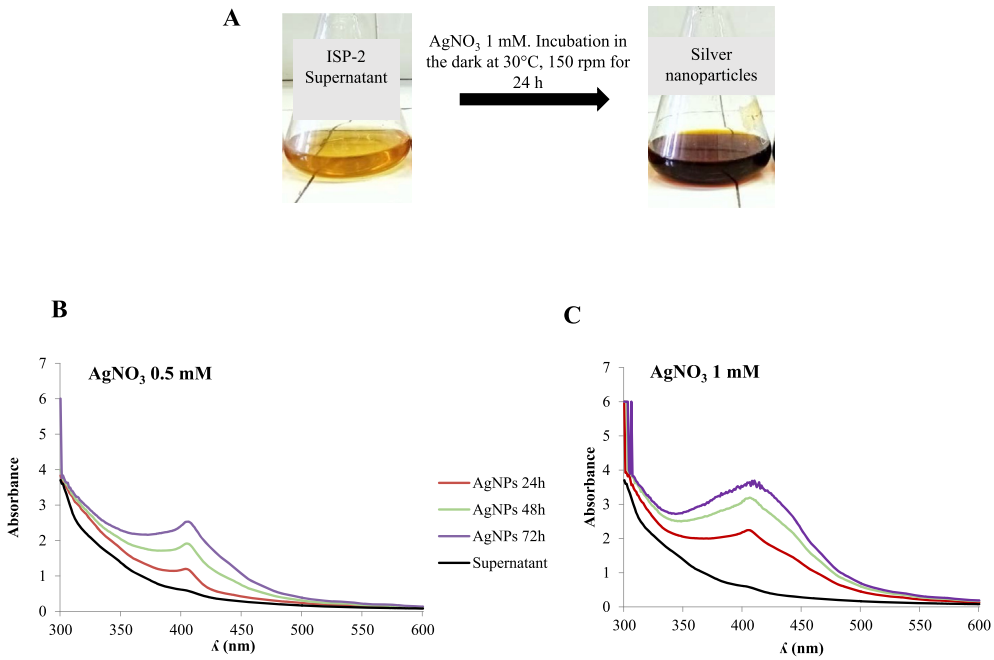

Figure 1. A: Yellowish-brown color of AgNPs synthesized by *Amycolatopsis tucumanensis*. B: UV–visible spectra of AgNPs synthesized by secondary metabolites of *A. tucumanensis.*

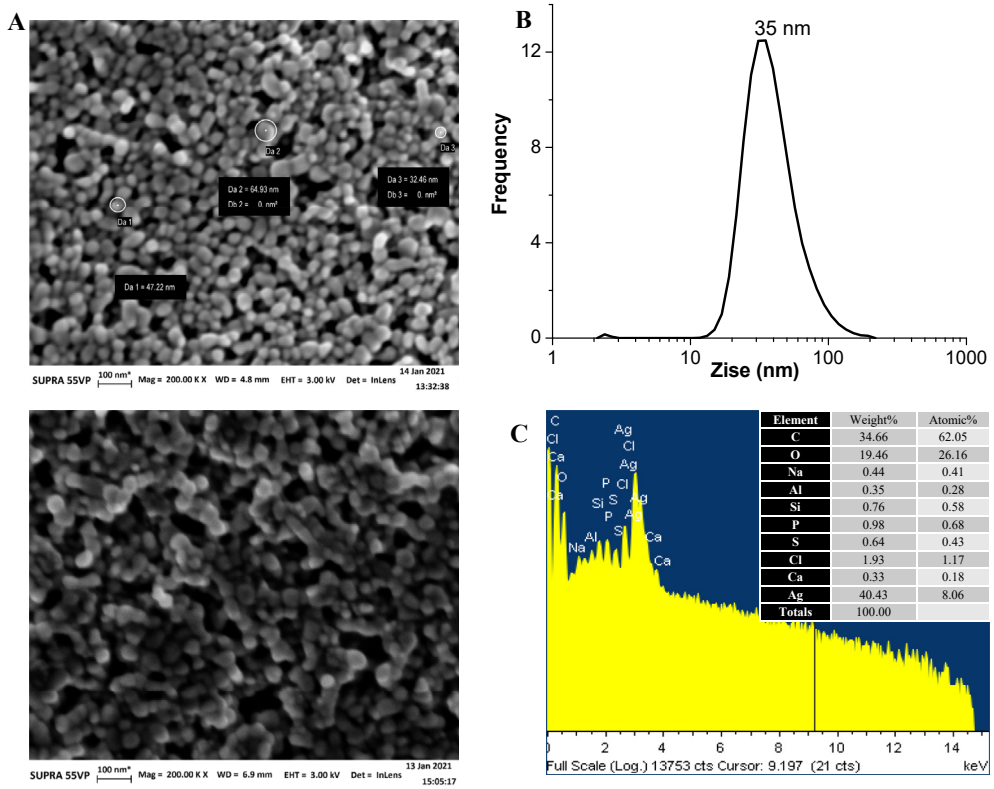

Figure 2. A: Scanning Electron Microscopy (SEM) images of spherical silver nanoparticles synthesized by *Amycolatopsis tucumanensis*. B: Particle size distribution and average diameter. Dynamic light scattering (DLS) measurement. C: Energy-Dispersive Spectroscopy (EDS) analysis, the major components of the nanoparticles were silver, carbon and oxygen.

XRD pattern clearly shows that the AgNPs formed by the reduction of Ag^{+} ions by *A. tucumanensis* are metallic (Ag^{0}) and crystalline in nature. Similar XRD patterns were observed in previous works where the crystalline structure of AgNPs was confirmed (Philip 2009; Shankar et al., 2003; Singh et al., 2021).

The functional organic groups of molecules associated with the AgNPs were determined by FTIR and Raman (Figures 4 and 5). The FTIR spectrum of AgNPs showed a peak at 1636 cm^{-1} suggesting the presence of amide I group associated to proteins (Figure 4A). The peak for amide I group was also observed with a smooth scrolling (1628 cm^{-1}) in the

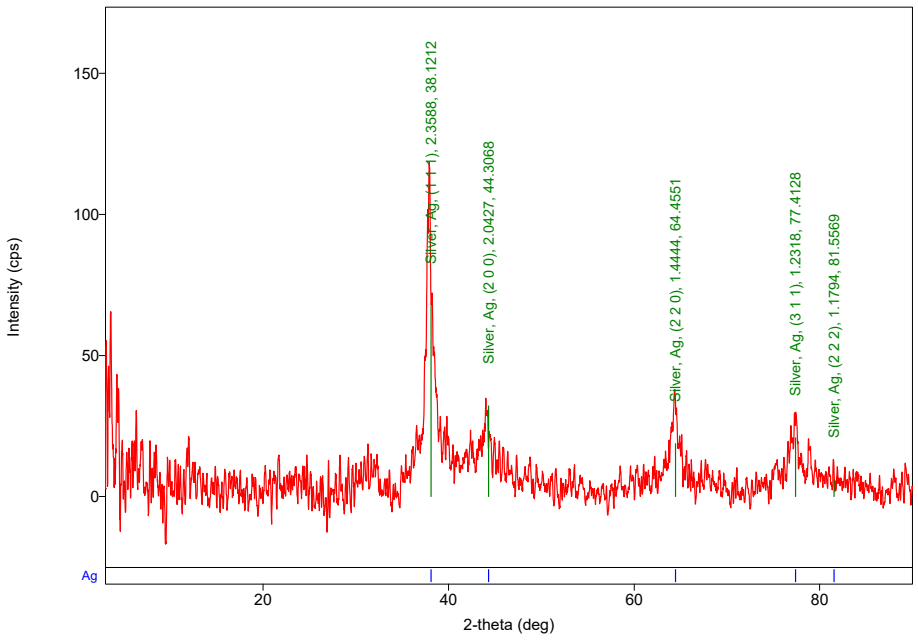

Figure 3. X-ray diffraction pattern of silver nanoparticles.

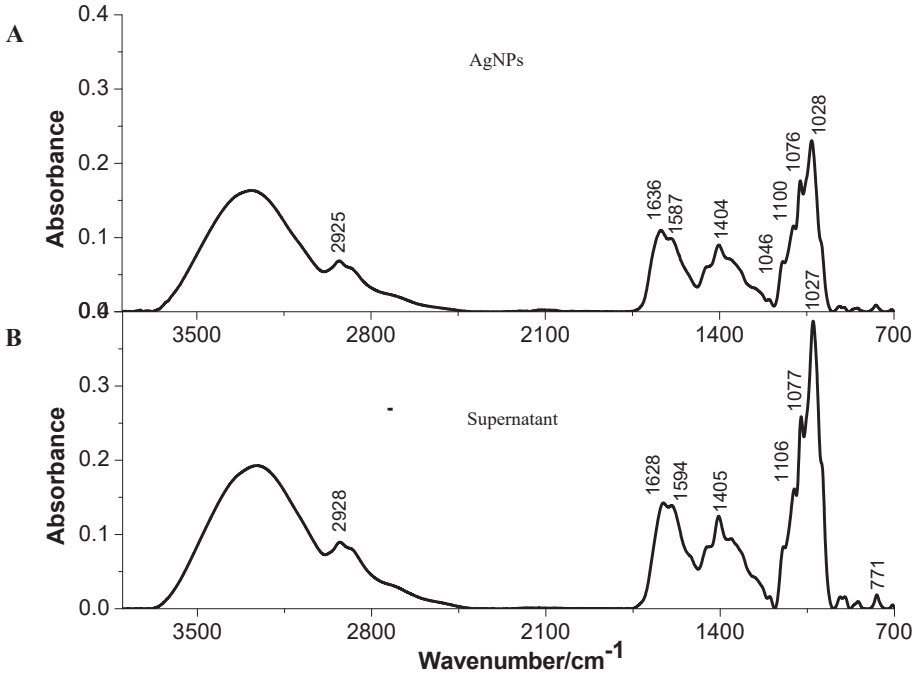

Figure 4. Fourier transform infrared (FT-IR) spectra of silver nanoparticles (A) and the supernatant where nanoparticles were synthesized (B).

supernatant where AgNPs were synthesized (Figure 4B). In addition, peaks that belong to the vibration of amide II group were observed at 1587 and 1594 cm^{-1} in the AgNPs and the supernatant respectively (Figures 4A and 4B). The absorption bands observed in both spectra at 2925-2928 cm^{-1} and 1076-1077 cm^{-1} indicate the presence of aromatic C–H and C=C bending (Figures 4A and 4B). Raman spectra of AgNPs and supernatant were recorded at two absorption regions: 532 and 785 nm (Figures 5A and 5B). In the Raman spectrum of AgNPs at 532, the peaks observed between 987 and 567 cm^{-1}, confirmed the C–H and C=C modes (Figure 5A). In the spectrum recorded at 785 nm, AgNPs showed a signal at 216 cm^{-1} attributed to the stretching vibrations of Ag–O bonds (Figure 5B). Besides, the signals observed at 1461 and 1367 cm^{-1} are related to amide II groups (Figure 5B). These results were consistent with previous FTIR and Raman analysis of AgNPs (Bakhtiari-Sardari et al., 2020; Paterlini et al., 2021; Zhang et al., 2016).

Organic molecules produced by the microorganisms during the primary and secondary metabolism usually have specific functions in the growth, proliferation and survival of the cells in the environment (Dávila Costa et al., 2021). In the green synthesis of AgNPs, these organic molecules are often involved in the reduction of the silver ions and stabilization of the nanoparticles (Roy et al., 2019; Zhang et al., 2020). In addition, these stabilizing or capping molecules were reported to improve the antimicrobial activity and avoid agglomeration of the nanoparticles. In a recent study, Paterlini et al. (2021) demonstrated that

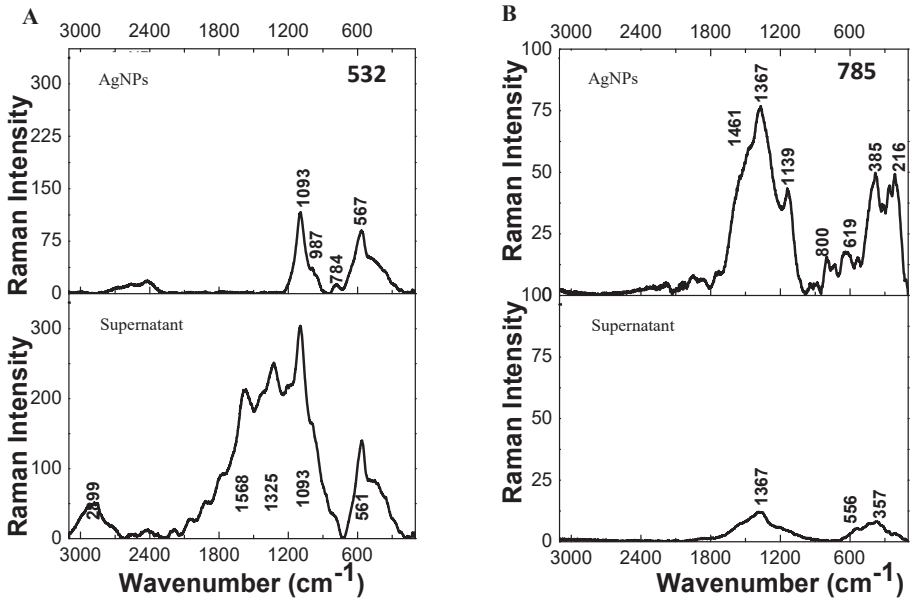

Figure 5. Raman spectra of silver nanoparticles and the supernatant where nanoparticles were synthesized. Spectra were recorded in the absorption regions: 532 nm (A) and 785 nm (B).

AgNPs synthetized by the strain *Streptomyces* sp. M7 are associated to aminopeptidases, transaldolases, tyrosinases and NAD(P)-dependent oxidoreductases. These proteins of the surface of the AgNPs are disposed in different layers and play a key role in the stabilization (Paterlini et al., 2021). In our study, EDS, FTIR and Raman spectra showed that organic molecules are associated to the surface of the AgNPs synthesized by *A. tucumanensis*. Undoubtedly, these organic molecules are involved in the stabilization of the AgNPs. Further omics studies will be conducted in order to elucidate the structure of these molecules.

The zeta potential is an indicator of the nanoparticles stability in aqueous suspensions. The value of zeta potential obtained for the AgNPs after one month of storage in distilled water was -48.2 ± 4.4mV. According to the literature, nanoparticles with a potential lower than −30 mV are very stable (Erdogan et al., 2019). This result also supports the hypothesis that organic molecules, whose functional groups were observed in the FTIR and Raman spectra, stabilize the AgNPs synthetized by *A. tucumanensis*.

3.3. Silver nanoparticles inhibited the growth of the phytopathogenic strain *Acidovorax avenae subsp. avenae*

AgNPs produced by *A. tucumanensis* were tested against *A. avenae* subsp. *avenae* by the well-diffusion method and subsequently the MIC was determined using the broth dilution method. Overall, AgNPs efficiently inhibited the growth of *A. avenue* subsp. *avenae*. The antimicrobial effect increased with the concentration of AgNPs. The major inhibition halo (18.5 mm) was observed at 80 μg/mL of AgNPs (Figure 6). However, in the presence of 40 and 8 μg/mL of AgNPs the growth of *A. avenue* subsp. *avenae* was also significantly inhibited as compared with the control (cell-free supernatant) (Figure 6). The MIC of AgNPs to inhibit the growth of *A. avenue* subsp. *avenae* was 20 μg/mL (see Supplementary materials). In a recent study, 20 μg/mL of AgNPs synthesized from fruit extract of *Phyllanthus emblica*, ranging in size from 19.8 to 92.8 nm, inhibited the growth of the rice pathogenic bacteria *Acidovorax oryzae* (Masum et al., 2019). In addition, Kaur et al. (2018) showed that 100 μg/mL of AgNPs (size 20–50 nm) synthesized by rhizospheric microflora of chickpea inhibited the growth of *Fusarium oxysporum* that causes the wilt disease of chickpea (Kaur et al., 2018). Unlike antibiotics, nanoparticles do not target specific traits of bacteria. Antibiotic resistance is often a modification of these traits. AgNPs may exert their toxicity through different mechanisms. Probably, the most important is the formation of reactive oxygen species. The surface-reactive groups of nanoparticles may interact with molecular oxygen and lead to formation of superoxide radical, hydrogen peroxide and hydroxyl radical leading to oxidative stress (Buchman et al., 2019; Dávila Costa et al., 2020). Based on the results obtained with *A. avenae* subsp. *avenae* and considering that the red strip disease causes great losses in sugarcane crops, *in vivo* assays were performed.

3.4. Control of sugarcane red stripe disease by using silver nanoparticles

The potential disease protection of silver nanoparticles was evaluated *in vivo*. This assay was performed to analyze induced resistance and/or antibacterial effect in a susceptible sugarcane variety under controlled growth conditions. For the induced resistance effect against red stripe disease, plants were sprayed once with silver nanoparticles 3 days before inoculation (T2) with a virulent isolate of *A. avenae* subsp. *avenae* (Table 1). In the antibacterial effect assay, plants were sprayed with silver nanoparticles 2 (T3) or 5 (T4) days after inoculation with the bacterium. DSI and AUDPC values of inoculated plants are shown in Table 1. The AgNPs (Treatment 2) were capable of inducing significant disease protection against red stripe at 9 dai. Treatments 3 and 4 did not produce significant red stripe control as antibacterial (Table 1) (Figure 7).

The *in vivo* and *in vitro* assays showed an interesting correlation. In both assays, the AgNPs were able to control the growth of *A. avenae* subsp. *avenae* and red stripe. The foliar application of AgNPs to control different plant diseases was also studied. For instance, early blight disease in *Solanum lycopersicum* (tomato) and bird's eye spot disease in *Camellia sinensis* (tea) were efficiently controlled (Gnanamangai et al., 2017; Kumari et al., 2017). The negative effect of AgNPs in plant tissues was also reported (Yan and Chen, 2019). However, the extend of the negative effects often depends on the plant species, concentration of AgNPs and number of doses. The *in vivo* assay consisted of one application of 80 μg/mL and no negative effects were observed in the sugarcane tissues. So far, the only method reported for the control of red stripe in sugarcane was the use of the biostimulant PSP1, an extracellular protease produced by the strawberry fungal pathogen *Acremonium strictum* (Chalfoun et al., 2018). It is important to highlight that the *in vivo* and *in*

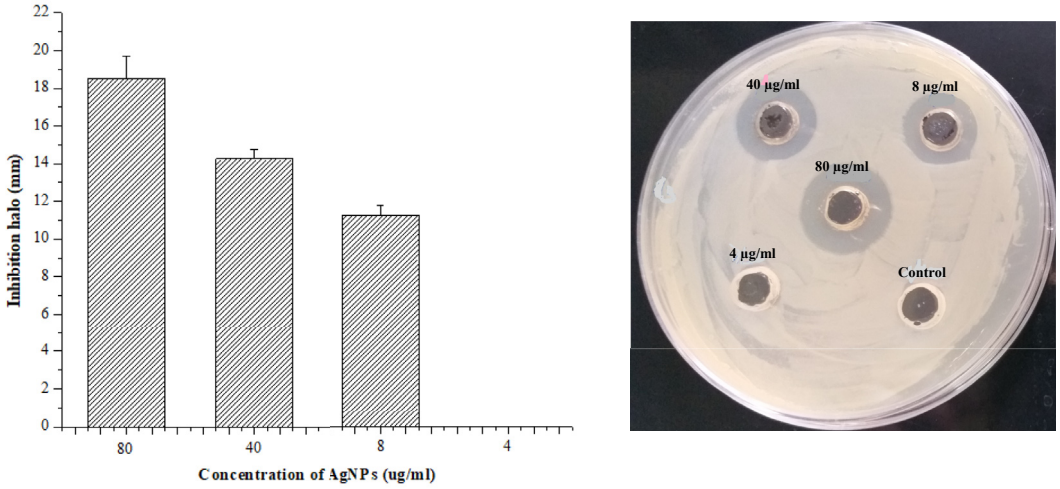

Figure 6. Antimicrobial activity against the sugarcane phytophatogen *Acidovorax avenae* subsp. *avenae*. Well-diffusion method using different concentration of silver nanoparticles (AgNPs). Control: cell-free supernatant.

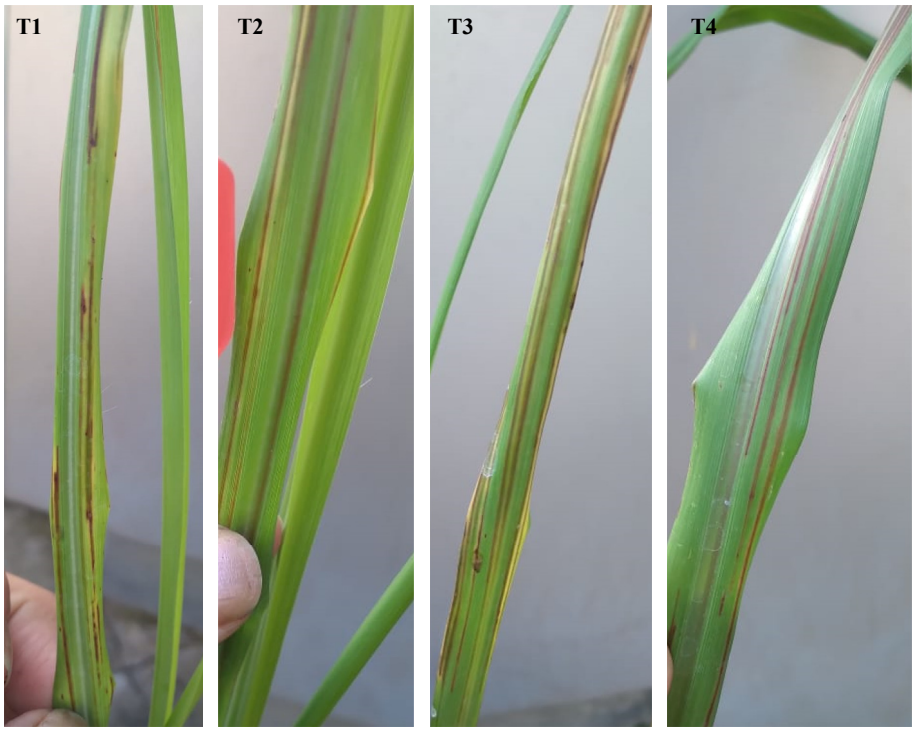

Figure 7. Typical red stripe disease symptoms in mock- and AgNPs-treated plants of red stripe susceptible variety (TUC 00–19) with a virulent strain of *A. avenae* subsp. *avenae*. (T1) Mock treatment, positive infection control. AgNPs treatments: applied 3 days before inoculation (T2), 2 days (T3) and 5 days (T4) after pathogen inoculation.

vitro assays performed in this work, represent the first report of biological AgNPs successfully used to control the growth of *A. avenae* subsp. *avenae* and red strip disease.

4. Conclusion

New molecules able to control diseases in value-added crops such as sugarcane are needed. In the present work, the strain *A. tucumanensis* was able to synthesize silver nanoparticles whose size was on average 35 nm. These nanoparticles inhibited the growth of the phytopathogen *A. avenae* subsp. *avenae* and demonstrated potential to control the red stripe disease in sugarcane. The extracellular mechanism of synthesis provided by *A. tucumanensis* and the not requirement of downstream processes do economically feasible the application of these nanoparticles at large scale. To our knowledge, this is the first report of AgNPs synthesized by a strain of the genus *Amycolatopsis* that controlled the red strip disease of sugarcane.

Declarations

Author contribution statement

Daiana S. Guerrero; Ana Ledesma; M. de los Angeles Frías: Performed the experiments.

Romina P. Bertani: Performed the experiments; Analyzed and interpreted the data; Wrote the paper.

Cintia M. Romero: Conceived and designed the experiments; Analyzed and interpreted the data.

José S. Dávila Costa: Conceived and designed the experiments; Analyzed and interpreted the data; Wrote the paper.

Funding statement

This work was supported by Fondo para la Investigación Científica y Tecnológica, PICT-2019-00742.

Data availability statement

Data included in article/supplementary material/referenced in article.

Declaration of interests statement

The authors declare no conflict of interest.

Additional information

Supplementary content related to this article has been published online at https://doi.org/10.1016/j.heliyon.2022.e09472.

References

Ahmed, T., Shahid, M., Noman, M., Niazi, M.B.K., Mahmood, F., Manzoor, I., Zhang, Y., Li, B., Yang, Y., Yan, C., Chen, J., 2020. Silver nanoparticles synthesized by using *Bacillus cereus* SZT1 ameliorated the damage of bacterial leaf blight pathogen in rice. Pathogens 9. Page 160 9, 160.

Albarracín, V.H., Amoroso, M.J., Abate, C.M., 2010. Bioaugmentation of copper polluted soil microcosms with *Amycolatopsis tucumanensis* to diminish phytoavailable copper for *Zea mays* plants. Chemosphere 79, 131–137.

Albarracín, V.H., Amoroso, M.J., Abate, C.M., 2005. Isolation and characterization of indigenous copper-resistant actinomycete strains. Chem. Erde - Geochem. 65, 145–156.

Argentina. Biofuels annual | USDA Foreign agricultural Service [WWW Document], n.d. URL. https://www.fas.usda.gov/data/argentina-biofuels-annual-6 (accessed 1.4.2022).

Asghari, F., Jahanshiri, Z., Imani, M., Shams-Ghahfarokhi, M., Razzaghi-Abyaneh, M., 2016. Antifungal nanomaterials: synthesis, properties, and applications. In: Nanobiomaterials in Antimicrobial Therapy: Applications of Nanobiomaterials. Elsevier, pp. 343–383.

Bakhtiari-Sardari, A., Mashreghi, M., Eshghi, H., Behnam-Rasouli, F., Lashani, E., Shahnavaz, B., 2020. Comparative evaluation of silver nanoparticles biosynthesis by two cold-tolerant *Streptomyces* strains and their biological activities. Biotechnol. Lett. 42, 1985–1999.

Bansal, P., Kaur, P., Singh Duhan, J., 2017a. Biogenesis of silver nanoparticles using *Fusarium pallidoroseum* and its potential against human pathogens. Ann. Biol. 33, 180–185.

Bansal, P., Kaur, P., Surekha Kumar, A., Duhan, J.S., 2017b. Microwave assisted quick synthesis method of silver nanoparticles using citrus hybrid "Kinnow" and its potential against early blight of tomato. Res. Crop. 18, 650–655.

Bertani, R., Joya, M., Henriquez, D., Funes, C., González, V., Perera, M., Cuenya, M., Castagnaro, A., 2020. Assessment of inoculation techniques for screening sugarcane resistance to red stripe disease caused by *Acidovorax avenae* subsp. *avenae*. AJCS 14, 1835–2707.

Bertani, R.P., Perera, M.F., Joya, C.M., Henriquez, D.D., Funes, C., Chaves, S., González, V., Welin, B., Cuenya, M.I., Castagnaro, A.P., 2021. Genetic diversity and population structure of *Acidovorax avenae* subsp. *avenae* isolated from sugarcane in Argentina. Plant Pathol. ppa.13413.

Bourguignon, N., Bargiela, R., Rojo, D., Chernikova, T.N., de Rodas, S.A.L., García-Cantalejo, J., Näther, D.J., Golyshin, P.N., Barbas, C., Ferrero, M., Ferrer, M., 2016. Insights into the degradation capacities of *Amycolatopsis tucumanensis* DSM 45259 guided by microarray data. World J. Microbiol. Biotechnol. 32.

Bourguignon, N., Irazusta, V., Isaac, P., Estévez, C., Maizel, D., Ferrero, M.A., 2019. Identification of proteins induced by polycyclic aromatic hydrocarbon and proposal of the phenanthrene catabolic pathway in *Amycolatopsis tucumanensis* DSM 45259. Ecotoxicol. Environ. Saf. 175, 19–28.

Brigida, A.B.S., Rojas, C.A., Grativol, C., Armas, E.M. de, Entenza, J.O.P., Thiebaut, F., Lima, M. de F., Farrinelli, L., Hemerly, A.S., Lifschitz, S., Ferreira, P.C.G., 2016. Sugarcane transcriptome analysis in response to infection caused by *Acidovorax avenae* subsp. *avenae*. PLoS One 11, e0166473.

Buchman, J.T., Hudson-Smith, N.V., Landy, K.M., Haynes, C.L., 2019. Understanding nanoparticle toxicity mechanisms to inform redesign strategies to reduce environmental impact. Acc. Chem. Res. 52, 1632–1642.

Campbell, C., 1990. Introduction to Plant Disease Epidemiology. Wiley, New York.

Cuenya, M., Chavanne, E., Ostengo, S., Garcia, M., Costilla, D., Ahmed, M., Dıaz Romero, C., Espinosa, M., Díaz, J., Delgado, N., 2013. TUC 00–19:una nueva variedad de caña de azúcar altamente productiva y demaduración temprana. Gac. Agroindust.

Dávila Costa, J.S., Albarracín, V.H., Abate, C.M., 2011. Cupric reductase activity in copper-resistant *Amycolatopsis tucumanensis*. Water Air Soil Pollut. 216.

Dávila Costa, J.S., Amoroso, M.J., 2014. Current biotechnological applications of the genus *Amycolatopsis*. World J. Microbiol. Biotechnol. 307 (30), 1919–1926.

Dávila Costa, J.S., Guerrero, D.S., Romero, C.M., 2021. *Streptomyces*: Connecting Red-Nano and Grey Biotechnology fields.

Dávila Costa, J.S., Kothe, E., Abate, C.M., Amoroso, M.J., 2012. Unraveling the *Amycolatopsis tucumanensis* copper-resistome. Biometals 25.

Dávila Costa, J.S., Romero, C.M., Rasuk, M.C., Pereyra, J., Guerrero, D., Álvarez, A., 2020. Nanoparticles for New Pharmaceuticals: Metabolites from *Actinobacteria*. Springer, Cham, pp. 195–213.

Di Rienzo, J., Casanoves, F., Balzarini, M., Gonzalez, L., Tablada, M., Robledo, C., 2018. InfoStat Versión 2018 [WWW Document].

Eid, A.M., Fouda, A., Niedbała, G., Hassan, S.E.D., Salem, S.S., Abdo, A.M., Hetta, H.F., Shaheen, T.I., 2020. Endophytic *Streptomyces laurentii* mediated green synthesis of Ag-NPs with antibacterial and anticancer properties for developing functional textile fabric properties. Antibiotics 9, 1–18.

El-Naggar, N.E.A., Abdelwahed, N.A.M., Darwesh, O.M.M., 2014. Fabrication of biogenic antimicrobial silver nanoparticles by *Streptomyces aegyptia* NEAE 102 as eco-friendly nanofactory. J. Microbiol. Biotechnol. 24, 453–464.

Erdogan, O., Abbak, M., Demirbolat, G.M., Birtekocak, F., Aksel, M., Pasa, S., Cevik, O., 2019. Green synthesis of silver nanoparticles via *Cynara scolymus* leaf extracts: the characterization, anticancer potential with photodynamic therapy in MCF7 cells. PLoS One 14, e0216496.

Fontana, P.D., Rago, A.M., Fontana, C.A., Vignolo, G.M., Cocconcelli, P.S., Mariotti, J.A., 2013. Isolation and genetic characterization of *Acidovorax avenae* from red stripe infected sugarcane in Northwestern Argentina. Eur. J. Plant Pathol. 137, 525–534.

Gnanamangai, B.M., Ponmurugan, P., Jeeva, S.E., Manjukarunambika, K., Elango, V., Hemalatha, K., Kakati, J.P., Mohanraj, R., Prathap, S., 2017. Biosynthesised silver and copper nanoformulation as foliar spray to control bird's eye spot disease in tea plantations. IET Nanobiotechnol. 11, 917–928.

Golinska, P., Rathod, D., Wypij, M., Gupta, I., Składanowski, M., Paralikar, P., Dahm, H., Rai, M., 2017. Mycoendophytes as efficient synthesizers of bionanoparticles: nanoantimicrobials, mechanism, and cytotoxicity. Crit. Rev. Biotechnol.

Goodfellow, M., 2012. Phylum XXVI. Actinobacteria phyl. nov. In: Bergey's Manual® of Systematic Bacteriology. Springer New York, New York, NY, pp. 33–2028.

Ibrahim, E., Luo, J., Ahmed, T., Wu, W., Yan, C., Li, B., 2020. Biosynthesis of silver nanoparticles using onion endophytic bacterium and its antifungal activity against rice pathogen *Magnaporthe oryzae*. J. Fungi 6. Page 294 6, 294.

Jalab, J., Abdelwahed, W., Kitaz, A., Al-Kayali, R., 2021. Green synthesis of silver nanoparticles using aqueous extract of *Acacia cyanophylla* and its antibacterial activity. Heliyon 7, e08033.

Jeong, H., Sim, Y.M., Kim, H.J., Lee, D.-W., Lim, S.-K., Lee, S.J., 2013. Genome sequence of the vancomycin-producing *Amycolatopsis orientalis* subsp. *orientalis* strain KCTC 9412T. Genome Announc. 1.

Kafarski, P., 2012. Rainbow code of biotechnology. Science 811–816.

Kaur, P., Thakur, R., Duhan, J.S., Chaudhury, A., 2018. Management of wilt disease of chickpea in vivo by silver nanoparticles biosynthesized by rhizospheric microflora of chickpea (*Cicer arietinum*). J. Chem. Technol. Biotechnol. 93, 3233–3243.

Kumar, R., Najda, A., Duhan, J.S., Kumar, B., Chawla, P., Klepacka, J., Malawski, S., Sadh, P.K., Poonia, A.K., 2021. Assessment of antifungal efficacy and release behavior of fungicide-loaded chitosan-carrageenan nanoparticles against phytopathogenic fungi. Polymers 14.

Kumari, M., Pandey, S., Bhattacharya, A., Mishra, A., Nautiyal, C.S., 2017. Protective role of biosynthesized silver nanoparticles against early blight disease in *Solanum lycopersicum*. Plant Physiol. Biochem. PPB 121, 216–225.

Magudapathy, P., Gangopadhyay, P., Panigrahi, B.K., Nair, K.G.M., Dhara, S., 2001. Electrical transport studies of Ag nanoclusters embedded in glass matrix. Phys. B Condens. Matter 299, 142–146.

Masum, M.I., Siddiqa, M.M., Ali, K.A., Zhang, Y., Abdallah, Y., Ibrahim, E., Qiu, W., Yan, C., Li, B., 2019. Biogenic synthesis of silver nanoparticles using *Phyllanthus emblica* fruit extract and its inhibitory action against the pathogen *Acidovorax oryzae* strain RS-2 of rice bacterial brown stripe. Front. Microbiol. 10, 820.

Paterlini, P., Rodríguez, C., Ledesma, A., Pereyra, J., Dávila Costa, J.S., Álvarez, A., Romero, C.M., 2021. Characterization of biosynthesized silver nanoparticles from *Streptomyces* aqueous extract and evaluation of surface-capping proteins involved in the process. Nano-Struct. Nano-Obj. 26, 100755.

Philip, D., 2009. Biosynthesis of Au, Ag and Au–Ag nanoparticles using edible mushroom extract. Spectrochim. Acta Mol. Biomol. Spectrosc. 73, 374–381.

Rai, M., Gade, A., Yadav, A., 2011. Biogenic nanoparticles: an introduction to what they are, how they are synthesized and their applications. In: Metal Nanoparticles in Microbiology. Springer Berlin Heidelberg, pp. 1–14.

Ramakrishnan, B., Venkateswarlu, K., Sethunathan, N., Megharaj, M., 2019. Local applications but global implications: can pesticides drive microorganisms to develop antimicrobial resistance? Sci. Total Environ. 654, 177–189.

Rodríguez-Félix, F., López-Cota, A.G., Moreno-Vásquez, M.J., Graciano-Verdugo, A.Z., Quintero-Reyes, I.E., Del-Toro-Sánchez, C.L., Tapia-Hernández, J.A., 2021. Sustainable-green synthesis of silver nanoparticles using safflower (*Carthamus tinctorius L.*) waste extract and its antibacterial activity. Heliyon 7, e06923.

Rott, P., Davis, M.J., 2000. Red stripe (top rot). In: Rott, P., Bailey, R.A., Comstock, J.C., Croft BJ, S.A. (Eds.), A Guide to Sugarcane Diseases. CIRAD/ISSCT, Montpellier, France, pp. 58–62.

Roy, A., Bulut, O., Some, S., Mandal, A.K., Yilmaz, M.D., 2019. Green synthesis of silver nanoparticles: biomolecule-nanoparticle organizations targeting antimicrobial activity. RSC Adv. 9, 2673–2702.

Saravanan, A., Kumar, P.S., Karishma, S., Vo, D.V.N., Jeevanantham, S., Yaashikaa, P.R., George, C.S., 2021. A review on biosynthesis of metal nanoparticles and its environmental applications. Chemosphere 264, 128580.

Shankar, S., Ahmad, A., Sastry, M., 2003. Geranium leaf assisted biosynthesis of silver nanoparticles. Biotechnol. Prog. 19, 1627–1631.

Sharma, A., Kumar, V., Shahzad, B., Tanveer, M., Sidhu, G.P.S., Handa, N., Kohli, S.K., Yadav, P., Bali, A.S., Parihar, R.D., Dar, O.I., Singh, K., Jasrotia, S., Bakshi, P., Ramakrishnan, M., Kumar, S., Bhardwaj, R., Thukral, A.K., 2019. Worldwide pesticide usage and its impacts on ecosystem. SN Appl. Sci.

Sindhu, R., Pandey, A., Binod, P., 2015. Microbial diversity of nanoparticle biosynthesis. Bio-Nanopart. Biosynth. Sustain. Biotechnol. Implic. 187–203.

Singh, J., Tripathi, J., Sharma, M., Nagar, S., Sharma, A., 2021. Study of structural, optical properties and antibacterial effects of silver nanoparticles synthesized by green synthesis method. Mater. Today Proc. 46, 2294–2297.

Vaidyanathan, R., Gopalram, S., Kalishwaralal, K., Deepak, V., Pandian, S.R.K., Gurunathan, S., 2010. Enhanced silver nanoparticle synthesis by optimization of nitrate reductase activity. Colloids Surf. B Biointerfaces 75, 335–341.

Verma, M., Kaur, J., Kumar, M., Kumari, K., Saxena, A., Anand, S., Nigam, A., Ravi, V., Raghuvanshi, S., Khurana, P., Tyagi, A.K., Khurana, J.P., Lal, R., 2011. Whole genome sequence of the rifamycin B-producing strain *Amycolatopsis mediterranei* S699. J. Bacteriol. 193, 5562.

Wanarska, E., Maliszewska, I., 2019. The possible mechanism of the formation of silver nanoparticles by *Penicillium cyclopium*. Bioorg. Chem. 93, 102803.

Wiegand, I., Hilpert, K., Hancock, R.E.W., 2008. Agar and broth dilution methods to determine the minimal inhibitory concentration (MIC) of antimicrobial substances. Nat. Protoc. 3, 163–175.

Xu, X., Han, L., Zhao, L., Chen, X., Miao, C., Hu, L., Huang, X., Chen, Y., Li, Y., 2018. Echinosporin antibiotics isolated from *Amycolatopsis* strain and their antifungal activity against root-rot pathogens of the *Panax notoginseng*. Folia Microbiol. 642 (64), 171–175.

Yan, A., Chen, Z., 2019. Impacts of silver nanoparticles on plants: a focus on the phytotoxicity and underlying mechanism. Int. J. Mol. Sci. 20.

Yonzone, R., Soniya Devi, M., 2018. Red stripe/top rot disease of sugarcane: a review. Int. J. Curr. Microbiol. Appl. Sci. 7, 1469–1478.

Zhang, D., Ma, X.L., Gu, Y., Huang, H., Zhang, G.W., 2020. Green synthesis of metallic nanoparticles and their potential applications to treat cancer. Front. Chem. 8, 799.

Zhang, X.F., Liu, Z.G., Shen, W., Gurunathan, S., 2016. Silver nanoparticles: synthesis, characterization, properties, applications, and therapeutic approaches. Int. J. Mol. Sci. 17.

Zhou, J.R., Sun, H.D., Ali, A., Rott, P.C., Javed, T., Fu, H.Y., Gao, S.J., 2021. Quantitative proteomic analysis of the sugarcane defense responses incited by *Acidovorax avenae* subsp. *avenae* causing red stripe. Ind. Crop. Prod. 162, 113275.